Inorganic Chemistry

Communication

pubs.acs.org/IC

Revisiting $[(RSn^{IV})_6Sn^{III}{}_2S_{12}]$: Directed Synthesis, Crystal Transformation, and Luminescence Properties

Jens P. Eußner,[†] Beatrix E. K. Barth,[†] Uwe Justus,[†] Nils W. Rosemann,[‡] Sangam Chatterjee,[‡] and Stefanie Dehnen*,[†]

[†]Fachbereich Chemie and Wissenschaftliches Zentrum für Materialwissenschaften, Philipps-Universität Marburg, Hans-Meerwein Straße, 35043 Marburg, Germany

[‡]Fachbereich Physik and Wissenschaftliches Zentrum für Materialwissenschaften, Philipps-Universität Marburg, Renthof 5, 35032 Marburg, Germany

Supporting Information

ABSTRACT: We report the synthesis of the mixed-valence cluster $[(R^5Sn^{IV})_6Sn^{III}{}_2S_{12}]$ [**1**; $R^5 = CMe_2CH_2C(O)Me$] under optimization of the reaction conditions. A new crystalline form of **1** in the orthorhombic space group *Pbca* was found at 250 K, which undergoes crystal transformation into the known monoclinic one at lower temperature. Further, we have studied the luminescence properties of **1**. Time-resolved photoluminescence measurements confirm the lability of the tin−chalcogenide bonds to UV irradiation, while the organic ligands are much less affected by it.

After the first structural characterization of organotin sesquisulfides in 1968[1] and their closer investigations in 1987 by Berwe and Haas,[2] many organic substituents of different polarity, bulkiness, and functionality have been established for the first $[(RT)_xS_y]$ (T = Si, Ge, Sn) clusters. Since then, the spectrum of the organic moieties as well as their inorganic cores has been expanded concerning their size, functionality, shape, and connection modes.[3] The lability of tin−chalcogen bonds of organofunctionalized chalcogenido clusters is well portrayed in the literature[4] and contributes to new rearrangements inside the Sn/S cores of lately found clusters: $[(R^1Sn)_4Sn_2S_{10}]$ [$R^1 = CMe_2CH_2C(Me)NNHPh$],[5] $[(R^2Sn)_2(R^3SnS)S_4]$, $[(R^3Sn)_2SnS_4)_2S_2]$ [$R^2 = CMe_2CH_2C(Me)NNC(2\text{-}py)_2$; $R^3 = CMe_2CH_2C(Me)NHNC(2\text{-}py)_2$; py = *o*-$C_5H_4N$],[6] or $[(R^4Sn)_2SnS_4)_2S_2]$ [$R^4 = CMe_2CH_2C(Me)NNH_2$].[7] In these cases, the organic ligands influence the composition and structure of the inorganic core. We have also reported light-induced transformation reactions with the formation of T−T bonds, inter alia the formation of a mixed-valence compound with noradamantane-type structure containing a Ge^{III}−Ge^{III} bond forming out of the light-sensitive germanium sesquiselenide complex $[(R^5Ge)_4Se_6]$ [$R^5 = CMe_2CH_2C(O)Me$][8] or the homoleptic, paddlewheel-type complex $[(R^5Sn^{IV})_6Sn^{III}{}_2S_{12}]\cdot 0.93CH_2Cl_2\cdot 1.08H_2S$ (**1**·0.93CH_2Cl_2·1.08 H_2S; **1a**) with one central Sn^{III}−Sn^{III} dumbbell.[9] While optoelectronic properties of group 14 chalcogenides are intensively investigated, investigations about T/E complexes (E = S, Se, Te)[10] with T−T bonds are still quite rare, especially with more than one or two chalcogen atoms.[11] They show nonlinear-optical and semiconducting properties that are of interest in potential technical applications.[12]

In the following, we present an alternative synthetic approach, solid-state phase transition, and the photophysical properties in time-resolved photoluminescence (TRPL) of the mixed-valence organofunctionalized paddlewheel-like cluster $[(R^5Sn^{IV})_6Sn^{III}{}_2S_{12}]$ (**1**).

During the preparation of the title compound for further characterization, we varied and optimized the synthesis of both the precursor $[(R^5Sn)_4S_6]$ (**A**, 97%) and **1** (81%). The synthesis of **1** was achieved in a significantly different way from that reported in ref 9. Instead of a light-induced condensation of **A**, the latter was dissolved together with freshly distilled CS_2 in an approximate 3:1 ratio in dichloromethane and stirred for 24 h at room temperature. Upon layering of the yellow solution with *n*-hexane (1:1 by volume), yellow crystals in the morphology of pentagonal dodecahedra and prisms formed within 3 days (see Scheme 1). Analytical data of both compounds are identical with those reported in ref 9, except the occurrence of a second, new *pseudo*polymorph of **1** (as **1b**) as outlined below.

Scheme 1. New Experimental Access to 1 (as Compound 1b) from A

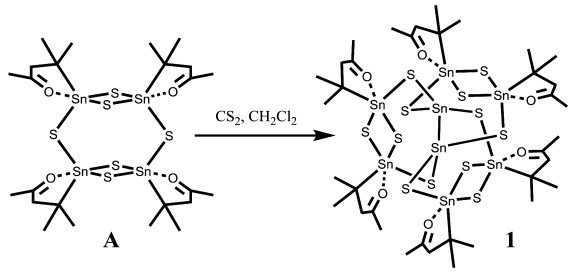

To rationalize the influence of carbon disulfide during the formation of **1** and give insights in the reaction, a series of experiments were done. The reaction requires a distinct excess of carbon disulfide. Lowering the amount of carbon disulfide drastically decreases the yield of the reaction, which rules out a catalytic activity of carbon disulfide during the formation of **1**. In

Received: October 30, 2014
Published: December 19, 2014

   dx.doi.org/10.1021/ic502627h | *Inorg. Chem.* 2015, 54, 22−24

contrast to the reported synthesis of **1** as **1a**, the exclusion of light did not affect the reaction. Neither the generation of molecular hydrogen in the atmosphere of the reaction vessel via gas chromatography nor the generation of mesityl oxide via ^{1}H and ^{13}C NMR spectroscopy were observed. ^{1}H NMR spectroscopy of the resulting yellow solution shows no clear indication of the other defined products; beneath sharp signals of **A** and **1**, broad small signals are present. To date, the mechanism of the formation of **1b** and the changed reaction conditions remain unknown. An intermediate generation of dithioesters might play a role[13] but has not been confirmed so far.

The changed crystallization conditions led to cocrystallization of two different *pseudo*polymorphs of **1** in a ca. 1:1 ratio. Besides the known monoclinic modification (**1a**, space group $P2_1/c$), which crystallizes as yellow pentagonal dodecahedra,[9] we observed yellow prisms of an orthorhombic *pseudo*polymorph (**1b**, space group *Pbca* at 250 K). Interestingly, cooling the orthorhombic crystals to 100 K induces a transformation of the crystal to the known monoclinic structure under twinning.[14] The structural parameters of both *pseudo*polymorphs are given in Table 1. The β angle in **1a** [90.56(3)°] is very close to 90°,

Table 1. Crystal Data of the Two *Pseudo*polymorphs in 1

	1a[9]	1b
cryst syst	monoclinic	orthorhombic
a/Å	23.971(7)	23.372(3)
b/Å	24.415(7)	24.291(2)
c/Å	23.174(7)	24.673(2)
β/deg; V/Å^3	90.56(3); 13562(7)	90; 14008(2)
space group, Z	$P2_1/c$, 8	*Pbca*, 8
T/K	100(2)	250(2)

indicating a very small difference between the two structures. This is also reflected in only a slight increase of the unit cell volume from 13562(7) Å^3 in **1a** to 14008(2) Å^3 in **1b**. The solid-state transformation in the monoclinic crystal system is irreversible. Warming up to room temperature does not reafford the orthorhombic form. In the light microscope, we observed that these crystals were torn into multiple domains.

In the orthorhombic modification, only one cluster is present in the asymmetric unit. The overall molecular structure within both structures is similar. Three $\{[(RSn)_2(\mu\text{-}S)_2]S_2\}$ units surround the central Sn^{III}–Sn^{III} unit with pseudo-C_{3h} symmetry. The Sn^{III}–Sn^{III} distance [2.802(1) Å], the Sn–S bond lengths [2.330(3)–2.531(3) Å], and the coordination by C,O bidentate organic ligands in **1b** are almost identical with those in **1a** within the accuracy of the method. The molecular structure of **1b** in the crystal is shown in Figure 1.

In both *pseudo*polymorphs, the organotin sulfide clusters are connected through weak C–H···O and C–H···S interactions. Because of heavy disorder of the solvent molecules CH_2Cl_2 and H_2S, the orthorhombic structure was refined with the solvent-free reflection data using the *SQUEEZE* routine. However, the squeezed data belong to an electron density of more solvent molecules than are present in **1a**. Thus, we assume that the transformation comes along with a loss of solvent molecules, probably upon cracking of the crystals, which agrees with the irreversibility. The relative orientation of the organic substituents shows small differences in both *pseudo*polymorphs (see Figure S3 in the SI) that come along with different intermolecular interactions. These were probably triggered or initiated by the loss of solvent, which we take as the driving force for the phase

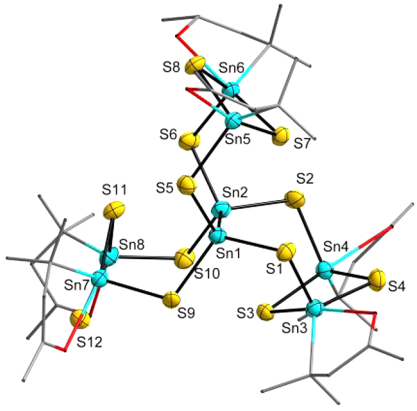

Figure 1. Molecular structure of **1b**. Ellipsoids are set with 30% probability (without disorder). Organic substituents are denoted as sticks and H atoms are omitted for clarity.

transformation. Some further examples for solid-state transitions from *Pbca* to $P2_1/c$ have been reported in the literature.[15]

To further characterize the compound, we performed TRPL measurements on single crystals of **1a**. A series of measurements for various excitation powers reveal the nature of the changes to the emission characteristics, e.g., by optically induced structural, morphological, or chemical changes. Therefore, we irradiated individual single crystals using 100 fs pulses at 3.5 eV and detected the emission in a streak-camera setup[16] with high spatial resolution including optical control. Typical images of crystals observed in our setup are depicted in the top row of Figure 2. Here, the white-light microscopy image (left) is shown next to the luminescent crystal for selective-area excitation (center). The outlines are marked in gray for reference. Large-area excitation of

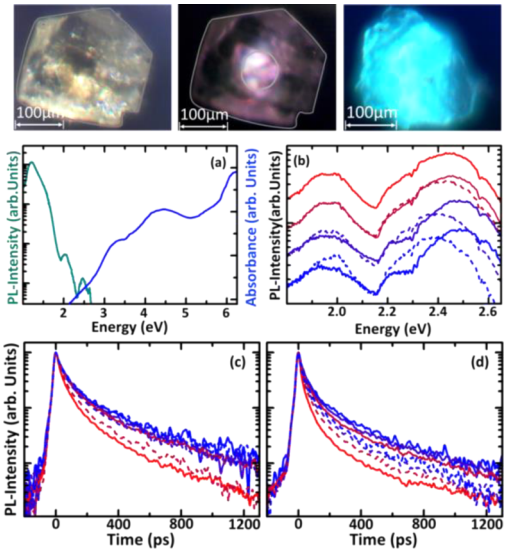

Figure 2. Top row: White-light microscopy image of a single crystal (left). Image for selective-area excitation, including a 3.3-eV-longpass filter in the imaging setup to block scattered pump laser light (crystal borders indicated by a gray line; center). A second crystal being homogeneously excited (right) with scattered pump laser. (a) Comparison of absorption and steady-state photoluminescence. (b) Normalized time-integrated photoluminescence spectra for pulsed UV excitation (curves vertically offset for clarity) and the corresponding time evolution of the lower-energy (c) and higher-energy (d) emission bands.

dx.doi.org/10.1021/ic502627h | *Inorg. Chem.* 2015, 54, 22–24

a whole crystal yields a glowing impression on the color charge-coupled device (right).

To analyze the nature of the emission bands, we plotted the time-integrated photoluminescence spectrum for continuous-wave excitation at 3.06 eV next to the linear absorption spectrum measured on a suspension of single crystallites in Nujol oil in Figure 2a. The emission is a virtually perfect mirror image of the absorbance, as expected according to the Franck−Condon principle. Thus, the highest-energy emission band at 2.40 eV is attributed to the charge-transfer relaxation from S to Sn atoms.[17] The transition at 1.94 eV is associated with relaxation of the ligand molecules to the ground state since the absorption band at 4.46 eV can be assigned to the corresponding n → π^* excitation.[9]

Next, we investigated the response of **1a** to high-power pulsed UV irradiation. Therefore, we plotted a series of normalized emission spectra in Figure 2b. The topmost curve was measured for 19 mW and the bottommost pair at 4 mW. The solid lines correspond to data taken for increasing powers, and the dotted ones were taken after the highest-power irradiation, i.e., when the power is reduced to the initial value again. Clearly, a pronounced red shift of the emission is found for the high-energy band at 2.4 eV.[3j] The lower-energy emission at 1.94 eV shows the same trend; however, the effect is much less pronounced. This behavior is typically regarded as a hallmark signature of optically induced defects. This interpretation is corroborated by the corresponding emission dynamics. We plot the spectrally integrated transients for the low- and high-energy bands in parts c and d of Figure 2c, respectively. Both bands show decreasing lifetimes with increasing excitation flux, with the latter recovering the initial values once the fluxes are ramped back down again. The higher-energy emission band remains significantly faster, as is expected if defects are formed.

We presented a new route into a mixed-valence organotin sulfide cluster and detected a solid-state phase transition from a new orthorhombic modification to the previously reported monoclinic one upon decreasing temperature. Furthermore, we have given conclusive evidence that the tin−chalcogenide bonds are selectively disturbed by UV irradiation, whereas the organic ligands remain widely unaffected.

■ ASSOCIATED CONTENT

Ⓢ Supporting Information

CIF, further details of syntheses, X-ray data, and TRPL measurements. This material is available free of charge via the Internet at http://pubs.acs.org.

■ AUTHOR INFORMATION

Corresponding Author

*E-mail: dehnen@chemie.uni-marburg.de. Fax: (+49) 6421-282-5653.

Author Contributions

The manuscript was written through contributions of all authors. All authors have given approval to the final version of the manuscript.

Notes

The authors declare no competing financial interest.

■ ACKNOWLEDGMENTS

This work was supported by the Deutsche Forschungsgemeinschaft within the framework of Grant GRK1782.

■ REFERENCES

(1) Dorfelt, C.; Janeck, A.; Kobelt, D.; Paulus, E. F.; Scherer, H. *J. Organomet. Chem.* **1968**, *14*, P22.

(2) Berwe, H.; Haas, A. *Chem. Ber.* **1987**, *120*, 1175.

(3) (a) Kobayashi, M.; Latour, S.; Wuest, J. D. *Organometallics* **1991**, *10*, 2908. (b) Ando, W.; Kadowaki, T.; Kabe, Y.; Ishii, M. *Angew. Chem., Int. Ed. Engl.* **1992**, *31*, 59. (c) Dakternieks, D.; Jurkschat, K.; Schollmeyer, D.; Wu, H. *J. Organomet. Chem.* **1995**, *492*, 145. (d) Choi, N.; Asano, K.; Watanabe, S.; Ando, W. *Phosphorus, Sulfur Silicon Relat. Elem.* **1997**, *120*, 379. (e) Herzog, U.; Rheinwald, G. *J. Organomet. Chem.* **2001**, *627*, 23. (f) Lange, H.; Herzog, U.; Borrmann, H.; Walfort, H. *J. Organomet. Chem.* **2004**, *689*, 4897. (g) Matsumoto, T.; Matsui, Y.; Ito, M.; Tatsumi, K. *Inorg. Chem.* **2008**, *47*, 1901. (h) Halvagar, M. R.; Hassanzadeh Fard, Z.; Dehnen, S. *Chem.—Eur. J.* **2011**, *17*, 4371. (i) Eußner, J. P.; Dehnen, S. *Chem. Commun.* **2014**, *50*, 11385. (j) Hassanzadeh Fard, Z.; Clérac, R.; Dehnen, S. *Chem.—Eur. J.* **2010**, *16*, 2050.

(4) (a) Dakternieks, D.; Jurkschat, K.; Wu, H.; Tiekink, E. R. T. *Organometallics* **1993**, *12*, 2788. (b) Wagner, M.; Zoller, T.; Hiller, W.; Prosenc, M. H.; Jurkschat, K. *Chem. Commun.* **2013**, *49*, 8925.

(5) Hassanzadeh Fard, Z.; Xiong, L.; Müller, C.; Hołyńska, M.; Dehnen, S. *Chem.—Eur. J.* **2009**, *15*, 6595.

(6) Barth, B. E. K.; Leusmann, E.; Harms, K.; Dehnen, S. *Chem. Commun.* **2013**, *49*, 6590.

(7) Eußner, J. P.; Barth, B. E. K.; Leusmann, E.; You, Z.; Rinn, N.; Dehnen, S. *Chem.—Eur. J.* **2013**, *19*, 13792.

(8) Heimann, S.; Hołyńska, M.; Dehnen, S. *Chem. Commun.* **2011**, *47*, 1881.

(9) Hassanzadeh Fard, Z.; Müller, C.; Harmening, T.; Pöttgen, R.; Dehnen, S. *Angew. Chem., Int. Ed.* **2009**, *48*, 4441.

(10) Dräger, M.; Mathiasch, B. *Z. Anorg. Allg. Chem.* **1980**, *470*, 45.

(11) (a) Dräger, M.; Häberle, K. *J. Organomet. Chem.* **1985**, *280*, 183. (b) Ando, W.; Tsumuraya, T. *Tetrahedron Lett.* **1986**, *27*, 3251. (c) Barrau, J.; Amine, J. E.; Rima, G.; Satgé, J. *Can. J. Chem.* **1986**, *64*, 615. (d) Puff, H.; Breuer, B.; Schuh, W.; Sievers, R.; Zimmer, R. *J. Organomet. Chem.* **1987**, *332*, 279. (e) Tsumuraya, T.; Sato, S.; Ando, W. *Organometallics* **1988**, *7*, 2015. (f) Tsumuraya, T.; Ando, W. *Organometallics* **1989**, *8*, 2286. (g) Brown, P.; Mahon, M. F.; Molloy, K. C. *J. Chem. Soc., Chem. Commun.* **1989**, 1621. (h) Schäfer, A.; Weidenbruch, M.; Saak, W.; Pohl, S.; Marsmann, H. *Angew. Chem., Int. Ed. Engl.* **1991**, *30*, 962. (i) Weidenbruch, M.; Ritschl, A.; Peters, K.; von Schnering, H. G. *J. Organomet. Chem.* **1992**, *438*, 39. (j) Weidenbruch, M.; Ritschl, A.; Peters, K.; von Schnering, H. G. *J. Organomet. Chem.* **1992**, *437*, C25.

(12) (a) Bowes, C. L.; Ozin, G. A. *Adv. Mater.* **1996**, *8*, 13. (b) Glitzendanner, R. L.; DiSalvo, F. J. *Inorg. Chem.* **1996**, *35*, 2623. (c) Kershaw, S. V.; Susha, A. S.; Rogach, A. L. *Chem. Soc. Rev.* **2013**, *42*, 3033. (d) Leusmann, E.; Wagner, M.; Rosemann, N. W.; Chatterjee, S.; Dehnen, S. *Inorg. Chem.* **2014**, *53*, 4228.

(13) McCormick, C. L.; Lowe, A. B. *Acc. Chem. Res.* **2004**, *37*, 312.

(14) Because of the nonmerohedral twinning, we only determined the cell parameters of the transformed crystal, which are in agreement with the known structural parameters of the monoclinic *pseudo*polymorph in ref 9 (we use the terminology *pseudo*polymorph because we cannot exclude that solvent is lost during the transformation). Crystallographic data for **1b** (M = 2044.94 g·mol^{-1}): orthorhombic space group *Pbca*, a = 23.372(3) Å, b = 24.291(2) Å, c = 24.673(2) Å, V = 14008(2) Å^3, Z = 8, ρ_{calc} = 1.939 g·cm^{-1}, μ = 3.299 mm^{-1}, 12256 reflections measured [R_{int} = 0.1312], 12256 unique reflections (the dataset was merged), 5108 with $I > 2\sigma(I)$, R1 = 0.0544 [$I > 2\sigma(I)$], wR2 = 0.1230 (all data), S = 0.718.

(15) (a) Vrcelj, R. M.; Clark, N. I. B.; Kennedy, A. R.; Sheen, D. B.; Shepherd, E. E. A.; Sherwood, J. N. *J. Pharm. Sci.* **2003**, *92*, 2069. (b) Chen, L.-Z.; Huang, D.-D.; Ge, J.-Z.; Wang, F.-M. *CrystEngComm* **2014**, *16*, 2944.

(16) Arbiol, J.; Magen, C.; Becker, P.; Jacopin, G.; Chernikov, A.; Schäfer, S.; Furtmayr, F.; Tchernycheva, M.; Rigutti, L.; Teubert, J.; Chatterjee, S.; Eickhoff, M. *Nanoscale* **2012**, *4*, 7517.

(17) Domingo, G.; Itoga, R.; Kannewurf, C. *Phys. Rev.* **1966**, *143* (2), 536.